

*Journal of*  
***Mechanics of***  
***Materials and Structures***

**ANALYSIS OF THE RUN-IN EFFECT IN FIBER-REINFORCED  
ISOLATORS UNDER VERTICAL LOAD**

James M. Kelly

***Volume 3, N° 7***

***September 2008***



mathematical sciences publishers



## **ANALYSIS OF THE RUN-IN EFFECT IN FIBER-REINFORCED ISOLATORS UNDER VERTICAL LOAD**

JAMES M. KELLY

Previous work on experimental and theoretical studies on fiber-reinforced bearings has shown the feasibility of using them as lightweight low-cost elastomeric isolators for application to housing, schools and other public buildings in highly seismic areas of the developing world. The theoretical analysis covered the mechanical characteristics of these bearings where the reinforcing elements, normally steel plates, are replaced by fiber reinforcement. The fiber in the fiber-reinforced isolator, in contrast to the steel in the conventional isolator (which is assumed to be rigid both in extension and flexure), is assumed to be flexible in extension, but completely without flexural rigidity. This leads to an extension of the theoretical analysis on which the design of steel-reinforced isolators is based that accommodates the stretching of the fiber-reinforcement. Several examples of isolators in the form of long strips were tested at the Earthquake Engineering Research Center Laboratory.

The theoretical analysis suggests, and the test results confirmed, that it is possible to produce a fiber-reinforced strip isolator that matches the behavior of a steel-reinforced isolator. The fiber-reinforced isolator is significantly lighter and can be made by a much less labor-intensive manufacturing process. The advantage of the strip isolator is that it can be easily used in buildings with masonry walls.

The main difference between the behavior of a fiber-reinforced and a steel-reinforced bearing is the degree of run-in under vertical loading. In this context we mean by run-in that a certain amount of vertical load must be applied to the bearing before its vertical stiffness can be developed.

The most likely source of the run-in is that the fibers are initially not straight and as they have no bending stiffness, the vertical stiffness cannot be developed until they have been straightened by the action of the applied vertical load. Straightening the fibers requires them to push against the surrounding rubber. This causes an increasing force in the fiber, and as it is straightening, there will be a transition to the stretching of the fiber and to the consequent stiffness of the composite system. These bearings can be used in a wide range of applications in addition to seismic protection of buildings including bridge bearings and vibration isolation bearings, so there is a need to be able to predict how much vertical load or vertical displacement is needed before the full vertical stiffness can be achieved. In this paper a theoretical analysis of the effect has been developed in an attempt to formulate a prediction for the transition from the initially bent to the finally straight fiber.

The method takes the already formulated analysis for the straight fiber and modifies it by treating the fiber as a curved string on an elastic foundation, adds to this an estimate of the subgrade reaction of this foundation, and, using the basic equations of the fiber-rubber composite, calculates the effective compression modulus as a function of the vertical compression strain or pressure.

### **1. Introduction**

The motivation for proposing the use of fiber-reinforced seismic isolators is the fact that the major loss of life in earthquakes happens when the event occurs in developing countries. Even in relatively moderate

---

*Keywords:* seismic isolation, fiber-reinforced isolators, elastomeric bearings, bearing mechanics.

earthquakes in areas with poor housing many people are killed by the collapse of brittle heavy unreinforced masonry or poorly constructed concrete buildings. Modern structural control technologies such as active control or energy dissipation devices can do little to alleviate this but it is possible that seismic isolation could be adopted to improve the seismic resistance of poor housing and other buildings such as schools and hospitals in developing countries. The possibility of using fiber-reinforced elastomeric isolators was reviewed by the author, Kelly [2002].

The problem with using isolation in developing countries is that conventional isolators are large, expensive and heavy. An individual isolator can weigh one ton or more and cost many thousands of dollars. To extend this earthquake-resistant strategy to housing and commercial buildings, the cost and weight of the isolators must be reduced.

The primary weight in an isolator is that of the steel reinforcing plates used to provide the vertical stiffness of the rubber-steel composite element. A typical rubber isolator has two large end-plates around 25 mm (1 inch) thick and 20 thin reinforcing plates around 3 mm (1/8 inch) thick. The high cost of producing the isolators reflects the labor involved in preparing the steel plates and laying-up of the rubber sheets and steel plates for vulcanization bonding in a mold. The steel plates are cut, sand blasted, acid cleaned and then coated with bonding compound. Next, the compounded rubber sheets with the interleaved steel plates are put into a mold and heated under pressure for several hours to complete the manufacturing process. Both the weight and the cost of isolators could be reduced if the steel reinforcing plates were eliminated and replaced by fiber reinforcement. As fiber materials are available with an elastic stiffness that is of the same order as that of steel, the reinforcement needed to provide the vertical stiffness may be obtained by using a similar volume of very much lighter material. There is also the fact that more steel is used than is needed to ensure the required vertical stiffness of the isolator because it is difficult to sand blast very thin plates. With carbon fiber, bonding can be done without this cleaning so that only the required minimum of reinforcement is needed. The cost savings may be possible if the use of fiber allows a simpler, less labor-intensive manufacturing process such as building the isolators in long rectangular strips, with individual isolators cut to the required size. All steel-reinforced isolators are currently manufactured as either circular or square. Rectangular isolators in the form of long strips would have distinct advantages over square or circular isolators when applied to buildings where the lateral-resisting system is walls. When isolation is applied to buildings with structural walls, additional wall beams are needed to carry the wall from isolator to isolator. A strip isolator would have a distinct advantage for retrofitting masonry structures and for isolating residential housing constructed from concrete or masonry blocks.

The vertical stiffness of a steel-reinforced bearing is approximated by assuming that each individual pad in the bearing deforms in such a way that horizontal planes remain horizontal and points on a vertical line lie on a parabola after loading. The plates are assumed to constrain the displacement at the top and bottom of the pad. Linear elastic behavior with incompressibility is assumed, with the additional assumption that the normal stress components are approximated by the pressure. This leads to the well-known pressure solution which is generally accepted as an adequate approximate approach for calculating the vertical stiffness. The extensional flexibility of the fiber reinforcement can be incorporated into this approach, and the resulting vertical stiffness calculated.

A number of carbon fiber-reinforced rubber strip isolators were tested on a small isolator test machine. The tests show that the concept is viable. The vertical and horizontal stiffnesses of the strip isolator are

less than those for the equivalent steel-reinforced isolator but still adequate and they proved to be easy to cut with a standard saw, in contrast to steel-reinforced isolators which are difficult to cut and need special saws. They are light and can be put in place without the use of lifting equipment.

While no fiber-reinforced isolators have been used to date in any building project the idea appears to have gained some attention in other countries. For example in Korea a group of researchers associated with Pusan University has studied the manufacturing of the bearings and their use for a shock absorbing system [Moon et al. 2003]. In Italy a group of researchers has tested rectangular carbon fiber-reinforced bearings as isolators for liquid storage tanks at refineries and petrochemical facilities [Summers et al. 2004]. Recent experimental work at McMaster University in Canada has confirmed that these bearings are a viable option for the base isolation of ordinary low-rise buildings [Toopchi-Nezhad et al. 2007]. All of this testing work indicates that these isolators are practical and it should lead to their widespread use.

## 2. Vertical stiffness of fiber-reinforced bearings

The essential characteristic of the elastomeric isolator is the very large ratio of the vertical stiffness to the horizontal stiffness. This is produced by the reinforcing plates, which in current industry standard are thin steel plates. These plates prevent lateral bulging of the rubber, but allow the rubber to shear freely. The vertical stiffness can be several hundred times the horizontal stiffness. The steel reinforcement has a similar effect on the resistance of the isolator to bending moments, referred to as the bending stiffness. This important design quantity makes the isolator stable against large vertical loads.

**2.1. Compression of pad with rigid reinforcement.** A linear elastic theory is the most common method used to predict the compression and the bending stiffness of a thin elastomeric pad. The first analysis of the compression stiffness was done using an energy approach by Rocard [1937]; further developments were made by Gent and Lindley [1959] and Gent and Meinecke [1970]. A very detailed description of the theory is given by Kelly [1996] and need not be repeated here. The analysis is an approximate one based on the kinematic assumptions that:

- (i) points on a vertical line before deformation lie on a parabola after loading;
- (ii) horizontal planes remain horizontal.

We consider an arbitrarily-shaped pad of thickness  $t$  and locate a rectangular Cartesian coordinate system,  $(x, y, z)$ , in the middle surface of the pad, as shown in Figure 1(a). Figure 1(b) shows the

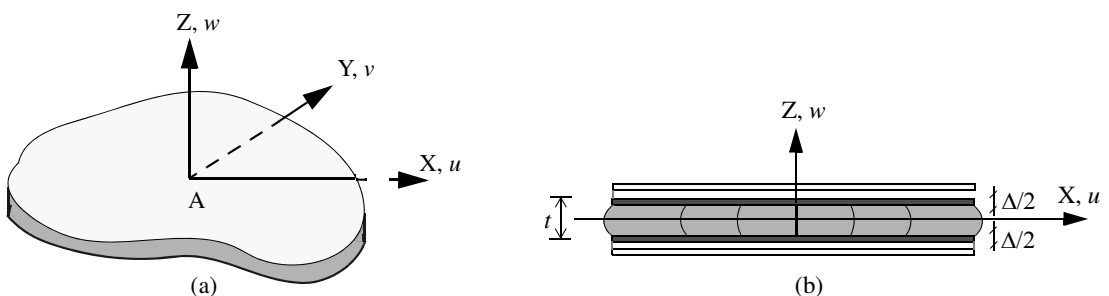


**Figure 1.** Constrained rubber pad and coordinate system.

displacements,  $(u, v, w)$ , in the coordinate directions under assumptions (i) and (ii):

$$\begin{aligned} u(x, y, z) &= u_0(x, y)(1 - 4z^2/t^2), \\ v(x, y, z) &= v_0(x, y)(1 - 4z^2/t^2), \\ w(x, y, z) &= w(z). \end{aligned} \tag{1}$$

This displacement field satisfies the constraint that the top and bottom surfaces of the pad are bonded to rigid substrates. The assumption of incompressibility produces a further constraint on the three components of strain,  $\epsilon_{xx}, \epsilon_{yy}, \epsilon_{zz}$ , in the form

$$\epsilon_{xx} + \epsilon_{yy} + \epsilon_{zz} = 0, \tag{2}$$

and this leads to

$$(u_{0,x} + v_{0,y})(1 - 4z^2/t^2) + w_{,z} = 0,$$

where the commas imply partial differentiation with respect to the indicated coordinate. When integrated through the thickness, this gives

$$u_{0,x} + v_{0,y} = \frac{3\Delta}{2t} = \frac{3}{2}\epsilon_c, \tag{3}$$

where the change of thickness of the pad is  $\Delta$  ( $\Delta > 0$  in compression), and  $\epsilon_c = \Delta/t$  is the compression strain.

The other assumptions of the theory are that the material is incompressible and that the stress state is dominated by the pressure,  $p$ , in the sense that the normal stress components can be taken as  $-p$ . The vertical shear stress components are included but the in-plane shear stress is assumed to be negligible.

These assumptions and the equations of stress equilibrium lead to the pressure solution

$$p_{,xx} + p_{,yy} = \nabla^2 p = -\frac{12G\Delta}{t^3} = -\frac{12G}{t^2}\epsilon_c. \tag{4}$$

The boundary condition,  $p = 0$ , on the perimeter of the pad completes the system for the pressure distribution,  $p(x, y)$ , across the pad. The effective compression modulus  $E_c$  of the pad is obtained by computing  $p(x, y)$  in terms of the compression strain  $\epsilon_c$ , and integrating it over the area of the pad to determine the resultant load  $P$ . The effective compression modulus is then given by

$$E_c = \frac{P}{A\epsilon_c}. \tag{5}$$

The value of  $E_c$  for a single rubber layer is controlled by the shape factor  $S$  defined as

$$S = \frac{\text{loaded area}}{\text{free area}},$$

which is a dimensionless measure of the aspect ratio of the single layer of the elastomer. For example, in an infinite strip of width  $2b$ , and with a single layer thickness of  $t$ ,  $S = b/t$ , and for a circular pad of diameter  $\Phi$  and thickness  $t$ ,  $S = \Phi/(4t)$ , and for a square pad of side  $a$  and thickness  $t$ ,  $S = a/(4t)$ .

In this paper we are only interested in the theory for a long strip when the effects of the ends can be neglected and the strip is taken to be infinite. For an infinite strip of width  $2b$  (see Figure 2), Equation

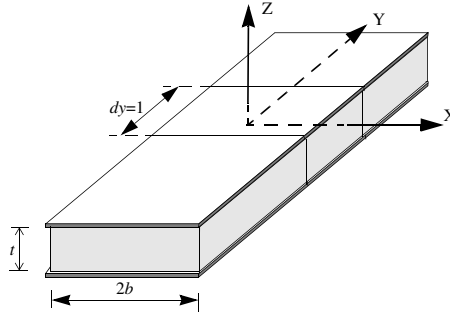


**Figure 2.** Infinitely long rectangular pad showing dimensions.

(4) reduces to

$$\nabla^2 p = \frac{d^2 p}{dx^2} = -\frac{12G}{t^2} \epsilon_c,$$

which, with  $p = 0$  at  $x = \pm b$ , gives

$$p = \frac{6G}{t^2} (b^2 - x^2) \epsilon_c.$$

In this case the load per unit length of the strip,  $P$ , is given by

$$P = \int_{-b}^b p \, dx = \frac{8Gb^3}{t^2} \epsilon_c. \tag{6}$$

Since the shape factor  $S$  is given by  $S = b/t$ , and the area per unit length is  $A = 2b$ ,

$$E_c = \frac{P}{A\epsilon_c} = 4GS^2. \tag{7}$$

**2.2. Compression stiffness with flexible reinforcement.** Before looking at the analysis for the bearing reinforced by fibers that are initially not straight it is necessary to review that for the initially straight fiber.

In developing the solution for the compression of a pad with flexible reinforcement, the rubber, as before, is assumed incompressible and the pressure is assumed to be the dominant stress component. The kinematic assumption of quadratically variable displacement is supplemented by an additional displacement that is constant through the thickness and is intended to accommodate the stretching of the reinforcement. Thus in this case the displacement pattern given in Equation (1) is replaced by

$$\begin{aligned} u(x, z) &= u_0(x)(1 - 4z^2/t^2) + u_1(x), \\ w(x, z) &= w(z), \end{aligned} \tag{8}$$

The constraint of incompressibility of Equation (2) remains, and, modified for the additional stretch of the reinforcement, becomes

$$u_{0,x} + \frac{3}{2}u_{1,x} = \frac{3\Delta}{2t}. \tag{9}$$

The only equation of stress equilibrium in this case is  $\sigma_{xx,x} + \tau_{xz,z} = 0$ , and the assumption of elastic behavior means that

$$\tau_{xz} = G\gamma_{xz}, \tag{10}$$

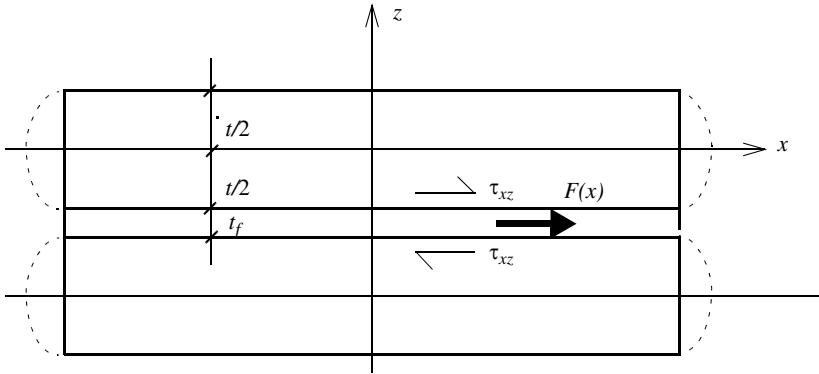


**Figure 3.** Force in equivalent sheet of reinforcement.

and calculating  $\gamma_{xz}$  from Equation (8) gives

$$\gamma_{xz} = -\frac{8z}{t^2}u_0. \tag{11}$$

The assumption that  $\sigma_{xx} = \sigma_{zz} = -p$ , when applied to the sole equation of equilibrium, provides

$$p_{,x} = -\frac{8Gu_0}{t^2}. \tag{12}$$

The individual fibers are replaced by an equivalent sheet of reinforcement of thickness  $t_f$ . The internal force,  $F(x)$ , per unit width of the equivalent reinforcing sheet is related to the shear stresses on the top and bottom of the pad by

$$\frac{dF}{dx} - \tau_{xz} \Big|_{z=t/2} + \tau_{xz} \Big|_{z=-t/2} = 0,$$

as shown in Figure 3. The shear stresses on the top and bottom of the pad are given by

$$\tau_{xz} \Big|_{z=t/2} = -\frac{4Gu_0}{t}, \quad \tau_{xz} \Big|_{z=-t/2} = \frac{4Gu_0}{t},$$

leading to

$$\frac{dF}{dx} = -\frac{8Gu_0}{t}. \tag{13}$$

When the fiber is assumed to be initially straight the extensional strain  $\epsilon_f$  in the reinforcement is related to the stretching force through the elastic modulus of the reinforcement  $E_f$  and the thickness  $t_f$  such that

$$\epsilon_f = u_{1,x} = \frac{F}{E_f t_f}, \tag{14}$$

which, when combined with Equation (13), gives

$$u_{1,xx} = -\frac{8G}{E_f t_f t}u_0. \tag{15}$$

The complete system to be solved consists of Equations (9), (12) and (15) above.

The boundary conditions used are the vanishing of the pressure  $p$  and the reinforcement force  $F$  at the edges of the strip,  $x = \pm b$  leading to  $p(\pm b) = 0, u_{1,x}(\pm b) = 0$ ; and the assumption of a symmetric

displacement pattern gives  $u_1(0) = 0, u_0(0) = 0$ . The results for  $p$  and  $F$  from [Kelly 1999] are

$$p = \frac{E_f t_f}{t} \left(1 - \frac{\cosh \alpha x / b}{\cosh \alpha}\right) \epsilon_c, \quad F(x) = E_f t_f \left(1 - \frac{\cosh \alpha x / b}{\cosh \alpha}\right) \epsilon_c, \tag{16}$$

where

$$\alpha^2 = \frac{12Gb^2}{E_f t_f t}. \tag{17}$$

The load per unit length of the strip,  $P$ , is given by

$$P = \frac{E_f t_f}{t} 2 \int_0^b \left(1 - \frac{\cosh \alpha x / b}{\cosh \alpha}\right) dx \epsilon_c = \frac{2E_f t_f}{\alpha t} b(\alpha - \tanh \alpha) \epsilon_c. \tag{18}$$

This result can be interpreted as an effective compression modulus,  $E_c$ , given by

$$E_c = \frac{E_f t_f}{t} \left(1 - \frac{\tanh \alpha}{\alpha}\right). \tag{19}$$

We note that when  $\alpha \rightarrow 0$ , i.e.,  $E_f \rightarrow \infty$ , we have  $E_c = 4GS^2$  as before. The formula also shows that  $E_c < 4GS^2$  for all finite values of  $E_f$ .

The effect of the elasticity of the reinforcement on  $E_c$  can be illustrated by normalizing the compression modulus  $E_c$ , by dividing by  $4GS^2$ , giving from Equation (19)

$$\frac{E_c}{4GS^2} = \frac{3}{\alpha^2} \left(1 - \frac{\tanh \alpha}{\alpha}\right), \tag{20}$$

which is shown in Figure 4 for  $0 \leq \alpha \leq 5$ . Note how the stiffness decreases with decreasing  $E_f$ .

It is worthwhile to note that  $\alpha$  also depends on the shape factor  $S$ , through

$$\alpha^2 = 12 \frac{G}{E_f} S^2 \frac{t}{t_f}.$$

In the case of carbon fiber reinforcement the ratio  $G/E_f$  will be extremely small although  $S^2$  and  $t/t_f$  are certain to be large.

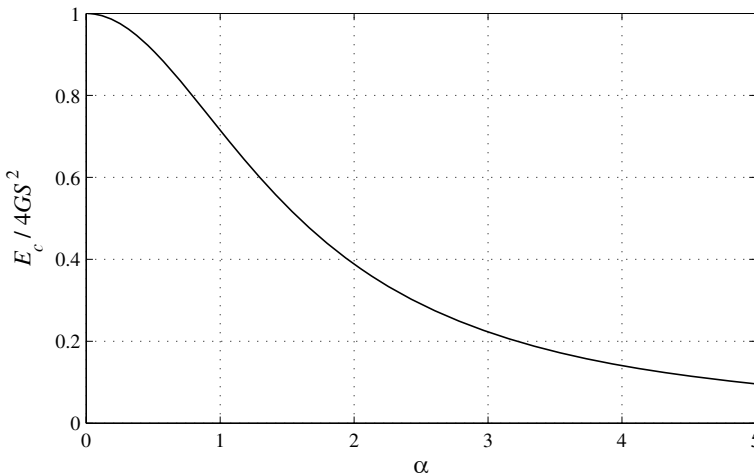


**Figure 4.** Normalized effective compression modulus as a function of  $\alpha = (12Gb^2/E_f t_f t)^{1/2}$ .

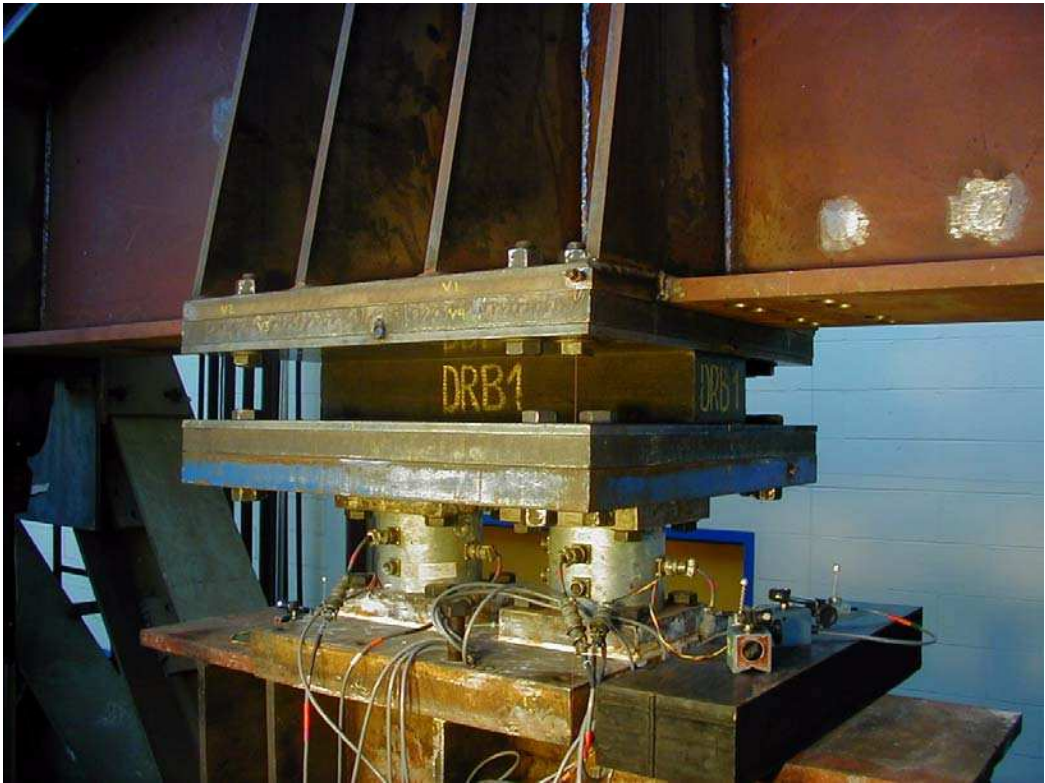


**Figure 5.** Fiber-reinforced bearing under vertical load.

**2.3. Analysis for initially imperfect fiber reinforcement.** There is one essential difference between the behavior of a fiber-reinforced bearing and a steel-reinforced bearing, and that is the degree of run-in before the full vertical stiffness is developed. In a steel-reinforced bearing the run-in is relatively small as shown in the examples in Figures 5, 6 and 7. In Figure 5 we see a fiber-reinforced bearing in the test machine under vertical load in this case generating a pressure of 6.9 MPa. The resultant force deflection curve is shown in Figure 6. The corresponding curve for a steel-reinforced bearing is shown in Figure 7. There is of course some run-in in this case but it is much less than that for the fiber bearing. It should be noted for comparison purposes that the steel bearing has much larger thickness of rubber. The steel plates are more or less rigid so their in-plane flexibility plays no role in the stiffness. The reason there is any run-in is probably that in the manufacturing process the plates are initially not quite parallel with the end plates and a slight amount of adjustment takes place as the vertical load is applied. In a fiber-reinforced bearing it is always much larger and one could speculate that the reason for this is that linear behavior is only developed when significant tension is produced in the fiber. This cannot be the explanation since if the fiber is straight it is its elastic extensibility that affects the vertical stiffness not the force in the fiber.

The most likely source of the run-in is that the fibers are initially not straight and as they have no bending stiffness, the vertical stiffness cannot be developed until they have been straightened by the action of the applied vertical load. Straightening the fibers requires the fiber to push against the surrounding rubber. This causes an increasing force in the fiber but as the fiber is straightening there will be a

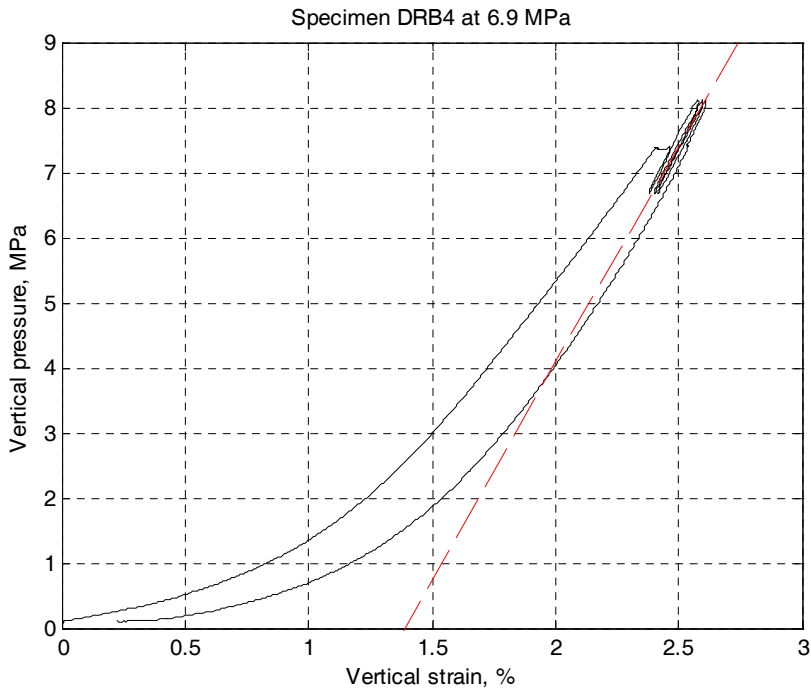


**Figure 6.** Pressure deflection curve for fiber bearing.

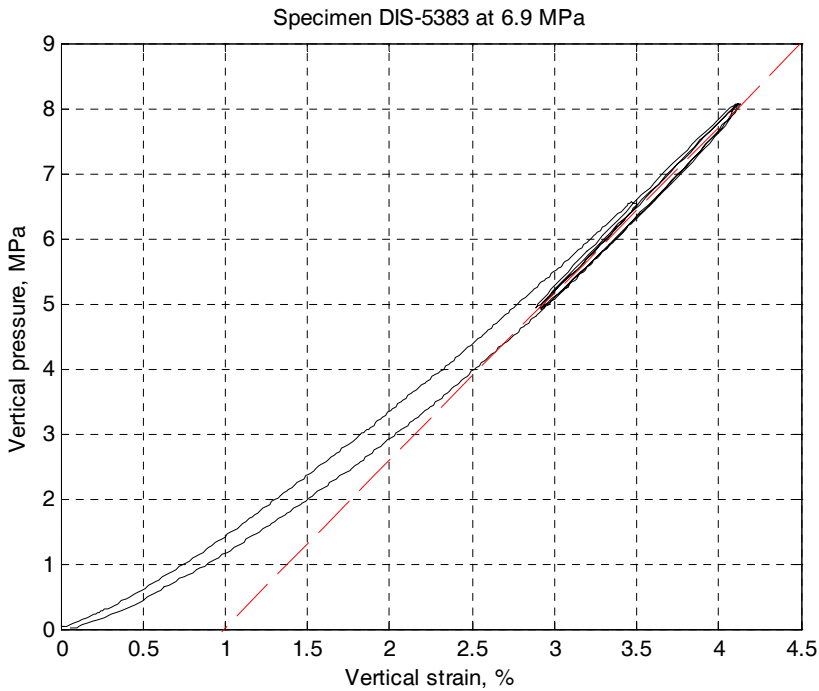


**Figure 7.** Pressure deflection curve for steel bearing.

transition to the tensile extensionality of the fiber and the consequent stiffness of the composite system. These bearings can be used in a wide range of applications including seismic protection of buildings, bridge bearings and vibration isolation bearings, so there is a need to develop a method for predicting how much vertical load or vertical displacement is needed before the full vertical stiffness can be achieved. The analysis here is an attempt to formulate a prediction for the transition from the initially bent to the finally straight fiber.

The method takes the already formulated analysis for the straight fiber and modifies it by treating the fiber as a string on an elastic foundation, adds to this an estimate of the subgrade reaction of this foundation, and, using the basic equations of the fiber-rubber composite, calculates the effective compression modulus as a function of the vertical compression strain.

If it is no longer assumed that the force in the fiber is related solely to the extensional strain as in Equation (14) the basic equations are Equations (4), (7) and (8) and a further constitutive equation for  $F$  is required, which will be derived in the next two sections.

**2.4. String on an elastic foundation.** The equation for the deflection  $v(x)$  of a tightly stretched string under the action of a lateral load  $p(x)$  is

$$T_0 \frac{d^2v}{dx^2} + p = 0,$$

where  $T_0$  is the constant  $x$ -component of the tension force in the string. The lateral load in this case is given by

$$p = k(v_0 - v),$$

where  $v_0$  is the initial shape of the string, giving as the equation for the deflection of the string

$$T_0 \frac{d^2v}{dx^2} - kv = kv_0.$$

If we assume that  $v_0(x) = v_0 \sin(\pi x/l)$  and  $v(x) = v \sin(\pi x/l)$  where now  $v_0$  and  $v$  are taken as constants we have

$$T_0 = k \frac{l^2(v_0 - v)}{\pi^2 v} \quad \text{or} \quad v = \frac{v_0}{1 + T_0 \pi^2 / (kl^2)},$$

showing that  $T_0 \rightarrow \infty$  as  $v \rightarrow 0$  and vice versa. The initial projected length of a half wavelength of the string is  $l$  and the curved length  $L$  is given by

$$L = l + \frac{1}{2} \int_0^l \left( \frac{d}{dx} v_0(x) \right)^2 dx.$$

We assume that the curved length remains constant so that as the string tension increases the deformed projected length increases to become  $l + \delta$ , such that

$$L = l + \delta + \frac{1}{2} \int_0^l \left( \frac{d}{dx} v(x) \right)^2 dx,$$

from which the change in length  $\delta$  becomes

$$\delta = \pi^2 \frac{(v_0^2 - v^2)}{4l},$$

and with  $v$  in terms of  $T_0$  and  $v_0$  from the above equation we have

$$\frac{\delta}{l} = \pi^2 \frac{v_0^2(2 + \pi^2 T_0/(kl^2))}{4l^2(1 + \pi^2 T_0/(kl^2))^2} \pi^2 \frac{T_0}{kl^2}.$$

To this result we add the stretch of the string due to its own elasticity, giving

$$\frac{\delta}{l} = \frac{T_0}{EA} + \pi^2 \frac{v_0^2(2 + \pi^2 T_0/(kl^2))}{4l^2(1 + \pi^2 T_0/(kl^2))^2} \pi^2 \frac{T_0}{kl^2}, \tag{21}$$

where  $E$  is the modulus of elasticity of the string and  $A$  is the cross sectional area.

At this point it is necessary to change from the variables of the string equations to the quantities of the fiber bearings. Thus  $T_0 \rightarrow F$ ,  $EA \rightarrow E_f t_f$  and  $\delta/l \rightarrow du_1/dx$ . We note that  $F$  now has the dimension of force/unit width and  $t_f$  is area/unit width.

**2.5. Estimation of subgrade stiffness between fiber and rubber.** We assume that the half-wavelength of the initial lack of straightness is much smaller than the thickness of the rubber layer and assume that the deformation takes place in a semiinfinite space and that the state of strain is plane strain. The material is assumed to incompressible.

Under these assumptions the stress strain relations

$$\epsilon_{xx} = \frac{1}{E} [(1 - \nu^2)\sigma_{xx} - \nu(1 + \nu)\sigma_{yy}], \quad \epsilon_{yy} = \frac{1}{E} [(1 - \nu^2)\sigma_{yy} - \nu(1 + \nu)\sigma_{xx}], \quad \gamma_{xy} = \frac{1}{G} \tau_{xy},$$

become

$$\epsilon_{xx} = \frac{1}{4G} [\sigma_{xx} - \sigma_{yy}], \tag{22}$$

$$\epsilon_{yy} = \frac{1}{4G} [\sigma_{yy} - \sigma_{xx}], \tag{23}$$

$$\gamma_{xy} = \frac{1}{G} \tau_{xy}. \tag{24}$$

The stress function  $\Phi$  given by

$$\frac{\partial^4}{\partial x^4} \Phi + 2 \frac{\partial^2}{\partial x^2} \frac{\partial^2}{\partial y^2} \Phi + \frac{\partial^4}{\partial y^4} \Phi = 0,$$

takes the form

$$\Phi = f(y) \sin \frac{\pi x}{l},$$

with

$$f = Ae^{\pi y/l} + Be^{-\pi y/l} + C \frac{\pi y}{l} e^{\pi y/l} + D \frac{\pi y}{l} e^{-\pi y/l},$$

where  $A$ ,  $B$ ,  $C$  and  $D$  are constants of integration. For a half space the constants  $A$  and  $C$  must vanish and  $\Phi$  reduces to

$$\Phi = \sin \frac{\pi x}{l} \left( Be^{-\pi y/l} + D \frac{\pi y}{l} e^{-\pi y/l} \right),$$

from which the stresses become

$$\begin{aligned} \sigma_{xx} &= \frac{\partial^2 \Phi}{\partial y^2} = \frac{\pi^2}{l^2} \sin \frac{\pi x}{l} \left( B - 2D + D \frac{\pi y}{l} \right) e^{-\pi y/l}, \\ \sigma_{yy} &= \frac{\partial^2 \Phi}{\partial x^2} = -\frac{\pi^2}{l^2} \sin \frac{\pi x}{l} \left( B + D \frac{\pi y}{l} \right) e^{-\pi y/l}, \\ \tau_{xy} &= \frac{\partial^2 \Phi}{\partial x \partial y} = \frac{\pi^2}{l^2} \cos \frac{\pi x}{l} \left( B - D + D \frac{\pi y}{l} \right) e^{-\pi y/l}. \end{aligned}$$

At the top surface,  $y = 0$ , we have  $\sigma_{yy} = p \sin(\pi x/l) = (-\pi^2/l^2) \sin(\pi x/l)B$  and  $\tau_{xy} = 0$ . Thus  $B = D = (l^2/\pi^2)p$  and the stresses become

$$\begin{aligned} \sigma_{xx} &= -p \sin \frac{\pi x}{l} \left( 1 - \frac{\pi y}{l} \right) e^{-\pi y/l}, \\ \sigma_{yy} &= -p \sin \frac{\pi x}{l} \left( 1 + \frac{\pi y}{l} \right) e^{-\pi y/l}, \\ \tau_{xy} &= p \cos \frac{\pi x}{l} \left( \frac{\pi y}{l} \right) e^{-\pi y/l}. \end{aligned}$$

To calculate the displacement field for these stresses we first calculate the strains which for the stress-strain relations from Equations (23), (24) and (25) are

$$\begin{aligned} \epsilon_{xx} &= \frac{p}{2G} \sin \frac{\pi x}{l} \left( \frac{\pi y}{l} \right) e^{-\pi y/l}, \\ \epsilon_{yy} &= -\frac{p}{2G} \sin \frac{\pi x}{l} \left( \frac{\pi y}{l} \right) e^{-\pi y/l}, \\ \gamma_{xy} &= \frac{p}{4G} \cos \frac{\pi x}{l} \left( \frac{\pi y}{l} \right) e^{-\pi y/l}. \end{aligned}$$

The resulting displacements obtained by integrating the strain-displacement equations for the first two are

$$\begin{aligned} u &= -\frac{p}{2G} \cos \frac{\pi x}{l} y e^{-\pi y/l} + f_1(y), \\ v &= \frac{p}{2G} \sin \frac{\pi x}{l} \left( 1 + \frac{\pi y}{l} \right) e^{-\pi y/l} + f_2(x), \end{aligned}$$

where at this point  $f_1(y)$  and  $f_2(x)$  are arbitrary functions of their respective variables. Substitution of these two displacement equations into the equation for the shear strain,

$$\gamma_{xy} = \frac{1}{G} \tau_{xy} = \frac{\partial u}{\partial y} + \frac{\partial v}{\partial x},$$

gives

$$\frac{p}{G} \cos \frac{\pi x}{l} y e^{-\pi y/l} + \frac{df_1}{dy} + \frac{df_2}{dx} = \frac{p}{G} \cos \frac{\pi x}{l} y e^{-\pi y/l},$$

from which we conclude that

$$\frac{df_1}{dy} + \frac{df_2}{dx} = 0,$$

and that the functions are equal and opposite constants, and the displacement field takes the form

$$u = -\frac{p}{2G} \cos \frac{\pi x}{l} y e^{-\pi y/l} + c,$$

$$v = \frac{p}{2G} \frac{l}{\pi} \sin \frac{\pi x}{l} \left(1 + \frac{\pi y}{l}\right) e^{-\pi y/l} - c,$$

It is reasonable to choose the upward displacement at the origin to be zero from which

$$v(0, 0) = 0 \text{ and } c = 0$$

and the displacement of the surface by the applied load is

$$v(x, 0) = \frac{p}{2G} \frac{l}{\pi} \sin \frac{\pi x}{l}.$$

In the context of the subgrade reaction we have  $p = k\delta$ , which, with

$$\delta = v\left(\frac{l}{2}, 0\right) = \frac{pl}{2G\pi},$$

leads finally to the result

$$k = 2G \frac{\pi}{l}. \tag{25}$$

In the bearing there is rubber on both sides of the fiber sheet so that the subgrade reaction will be twice this.

**2.6. Calculation of compression modulus.** The main purpose of this paper is to calculate the compression modulus  $E_c$  as a function of the compression strain  $\epsilon_c$  as the fiber is straightened from its initial imperfect condition. The procedure will be to calculate the tension force  $F$  in the fiber as a function of the compression strain and from that the pressure distribution  $p(x)$ , which, when integrated over the area of the bearing, gives the total compression load  $P$ . Knowing the load and the strain the modulus is calculated from

$$E_c = \frac{P}{A\epsilon_c}. \tag{26}$$

The basic equations for the fiber-reinforced strip bearing are repeated here to clarify the method. They are the constraint equation of incompressibility

$$\frac{du_0}{dx} + \frac{3}{2} \frac{du_1}{dx} = \frac{3}{2} \epsilon_c,$$

the equilibrium equation relating pressure and shear stress in the rubber

$$\frac{dp}{dx} = -\frac{8Gu_0}{t^2},$$

and the equilibrium equation for the tension force in the fiber

$$\frac{dF}{dx} = -\frac{8Gu_0}{t}.$$

Using the first equation to eliminate  $u_0$ , the third equation becomes

$$\frac{d^2 F}{dx^2} = \frac{12G}{t} \frac{du_1}{dx} - \frac{12G}{t} \epsilon_c.$$

For a straight fiber,  $du_1/dx$  is the tensile strain in the fiber and is related to  $F$  through the elasticity of the fiber, but here we use the expression for  $\delta/l$  from Equation (21), giving

$$\frac{d^2 F}{dx^2} - \frac{12G}{t} \left( \frac{F}{E_f t_f} + \frac{\pi^2 v_0^2}{4l^2} \frac{2 + F\pi^2/(kl^2)}{(1 + F\pi^2/(kl^2))^2} \right) = -\frac{12G}{t} \epsilon_c.$$

This can be written in terms of dimensionless groups of variables in the form

$$\frac{d^2}{dx^2} \left( \frac{F\pi^2}{kl^2} \right) - \frac{12G}{E_f t_f t} \left( 1 + E_f t_f \frac{\pi^2 v_0^2}{4l^2} \frac{\pi^2}{kl^2} \frac{2 + F\pi^2/(kl^2)}{(1 + F\pi^2/(kl^2))^2} \right) \frac{F\pi^2}{kl^2} = -\frac{12G}{t} \frac{\pi^2}{kl^2} \epsilon_c.$$

We note here that the subgrade reaction calculated in the previous section is now  $4\pi G/l$  since the fiber has rubber on both sides. It is now convenient to define the following set of dimensionless variables:

$$\bar{x} = \frac{x}{b}, \quad y = \frac{\pi F}{4Gl}, \quad \alpha^2 = \frac{12Gb^2}{E_f t_f t}, \quad \beta = \frac{\pi^3 v_0^2}{16Gl^3} E_f t_f, \quad s = 3\pi \frac{b^2}{tl} \epsilon_c. \tag{27}$$

In terms of these variables the complete system of equations reduces to

$$\frac{d^2 y}{d\bar{x}^2} - \alpha^2 \left( 1 + \beta \frac{2 + y}{(1 + y)^2} \right) y = -s, \tag{28}$$

on  $-1 \leq \bar{x} \leq 1$  with  $y(-1) = y(1) = 0$ . It is worth noting at this point that when  $s \rightarrow 0$  and  $y \rightarrow 0$ , this equation takes the form

$$\frac{d^2 y}{d\bar{x}^2} - \alpha^2 (1 + 2\beta) y = -s,$$

and if  $s$  is very large,  $y$  also becomes large and the term  $\beta(2 + y)/(1 + y)^2$  tends to zero, and the equation becomes

$$\frac{d^2 y}{d\bar{x}^2} - \alpha^2 y = -s.$$

When the fiber is initially straight, i.e.,  $\beta = 0$ , the latter equation prevails, demonstrating that the effect of the initial imperfection is subsumed in the  $\beta$  term.

**2.7. Solution Technique.** Equation (28), for  $y = y(x)$ , is essentially unsolvable except by numerical methods, but a good approximation can be obtained by replacing  $y(x)$  in the bracketed term by  $\bar{y}$  where,

$$\bar{y} = \frac{1}{2} \int_{-1}^1 y(\bar{x}) d\bar{x}.$$

We then solve

$$\frac{d^2 y}{d\bar{x}^2} - \bar{\alpha}^2 y = -s,$$

where

$$\bar{\alpha}^2 = \alpha^2 \left( 1 + \beta \frac{2 + \bar{y}}{(1 + \bar{y})^2} \right).$$

The solution using, symmetry and the boundary conditions at the edges,  $y(\pm 1) = 0$ , is

$$y = \frac{s}{\bar{\alpha}^2} \left( 1 - \frac{\cosh \bar{\alpha} \bar{x}}{\cosh \bar{\alpha}} \right),$$

and the corresponding result for  $\bar{y}$  is

$$\bar{y} = \frac{s}{\bar{\alpha}^2} \left( 1 - \frac{\tanh \bar{\alpha}}{\bar{\alpha}} \right),$$

finally giving as the equation for  $\bar{\alpha}$

$$\bar{\alpha}^2 = \alpha^2 \left( 1 + \beta \frac{2 + (s/\bar{\alpha}^2)(1 - (\tanh \bar{\alpha})/\bar{\alpha})}{(1 + (s/\bar{\alpha}^2)(1 - (\tanh \bar{\alpha})/\bar{\alpha}))^2} \right). \tag{29}$$

The solution technique is to now specify the bearing parameters  $\alpha^2$  and  $\beta$ , vary  $s$ , solve the equation for  $\bar{\alpha}^2$ , and, knowing this calculate first  $\bar{y}$  and then  $F(\bar{x})$  from

$$F(\bar{x}) = \frac{12Gb^2}{t} \frac{1}{\bar{\alpha}^2} \left( 1 - \frac{\cosh \bar{\alpha} \bar{x}}{\cosh \bar{\alpha}} \right) \epsilon_c.$$

From the basic equations for the fiber bearing we have

$$\frac{dp}{dx} = \frac{1}{t} \frac{dF}{dx},$$

giving

$$p(x) = \frac{1}{t} F(x) + A,$$

where  $A$  is a constant of integration. The boundary condition on  $p$  is  $p(b) = p(-b) = 0$ , but that for  $F$  is also  $F(b) = F(-b) = 0$ , so that  $A = 0$  and

$$p(\bar{x}) = \frac{12Gb^2}{t^2} \frac{1}{\bar{\alpha}^2} \left( 1 - \frac{\cosh \bar{\alpha} \bar{x}}{\cosh \bar{\alpha}} \right) \epsilon_c,$$

from which we have

$$P = \frac{12Gb^2}{t^2} \frac{2b}{\bar{\alpha}^2} \left( 1 - \frac{\tanh \bar{\alpha}}{\bar{\alpha}} \right) \epsilon_c = E_c(2b)\epsilon_c, \quad E_c = \frac{12Gb^2}{t^2} \frac{1}{\bar{\alpha}^2} \left( 1 - \frac{\tanh \bar{\alpha}}{\bar{\alpha}} \right).$$

Since  $S = b/t$ , this can be written in the form

$$E_c = 4GS^2 \frac{3}{\bar{\alpha}^2} \left( 1 - \frac{\tanh \bar{\alpha}}{\bar{\alpha}} \right), \tag{30}$$

where  $4GS^2$  is, we recall, the modulus of the steel-reinforced bearing.

**2.8. Orders of magnitude and numerical examples.** The important quantities for any particular solution are  $\alpha$  and  $\beta$ . We have

$$\alpha^2 = \frac{4GS^2 t}{E_f t_f}, \quad \beta = \frac{\pi^3 E_f v_0^2 t_f}{16G l^3}.$$

Typical properties for a fiber-reinforced bearing are  $S = 10$ ,  $G = 100$  psi,  $E_f = 20 \times 10^6$  psi and  $t/t_f = 10$ , from which we get  $\alpha \approx 0.25$ . To estimate the value of  $\beta$  we assume that the initial lack of straightness  $v_0$  is of order  $t_f$  and that there are 10 half-wavelengths across the width of an individual layer which gives a value of 400. The initial modulus is given by

$$E_c^0 = 4GS^2 \frac{3}{\alpha^2(1+2\beta)} \left(1 - \frac{\tanh \alpha(1+2\beta)^{1/2}}{\alpha(1+2\beta)^{1/2}}\right),$$

and the fully developed modulus by

$$E_c^\infty = 4GS^2 \frac{3}{\alpha^2} \left(1 - \frac{\tanh \alpha}{\alpha}\right).$$

For this selection of parameters the quantity  $\alpha(1+2\beta)^{1/2}$  takes the value 7.1 and the initial modulus is

$$E_c^0 = 4GS^2(0.0510),$$

and the asymptotic modulus is

$$E_c^\infty = 4GS^2(0.9756),$$

a ratio of about 19, showing how a small deviation from initial straightness can cause a very large reduction in the stiffness and presumably lead to the observed initial run-in before the full stiffness of the bearing is developed.

The question still to be resolved is the level of vertical compression needed to produce a straight fiber. To determine this it is necessary to calculate the evolution of  $E_c$  as a function of  $s$  from its initial value at  $s = 0$ . It should be recalled that  $s$  depends on  $\epsilon_c$  through Equation (27). For the parameters already used, we have  $s = 1000\epsilon_c$ . The process is now to insert values of  $s$  into Equation (29) calculate  $\bar{\alpha}$ , and then calculate  $E_c$  from Equation (30). To evaluate the average pressure on the surface of the bearing that is needed to achieve a certain value of the modulus it is only necessary to multiply the current value of  $E_c(\epsilon_c)$  by  $\epsilon_c$  to provide this information. A number of examples have been computed from the analysis, with the only difference between them being the degree of initial imperfection of the fiber. Thus we fix  $\alpha$  and vary  $s$  and calculate  $E_c$  in terms of  $\epsilon_c$  and then the average pressure  $p = E_c \epsilon_c$  for certain values of  $b$ . These examples are shown in Figure 8. It is clear that the initial lack of straightness can have a very large effect on the initial stiffness of the bearing but it is also clear that it is not necessary to have the fiber totally straight for the stiffness to achieve the effective final value.

It is worth noting that at this value of  $\alpha$  the effect of the flexibility of the fiber reinforcement is, if the fiber were straight, quite small; the reduction in the compression modulus is only 2.5% and one could speculate that the large effect of the initial lack of straightness could be due to this. To check if this in fact the case the results were computed for the example corresponding to a reduction of the fiber modulus by a factor of sixteen giving  $\alpha = 1.00$ . These results are shown in Figure 9. It is clear that even with a very flexible fiber the initial lack of stiffness still plays a major role in the evolution of the modulus and the load deflection curve.

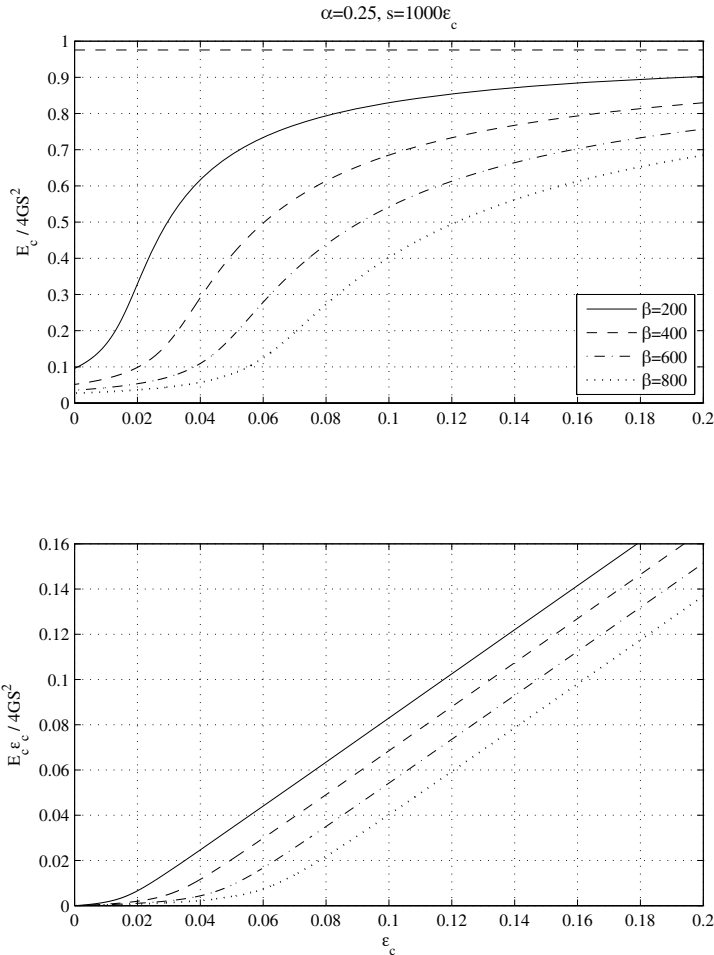


**Figure 8.** Run-in for high-stiffness fiber case: modulus and pressure vs. strain.

### 3. Conclusions

The main difference between the behavior of a fiber-reinforced and a steel-reinforced bearing is the degree of run-in under vertical loading. In this paper it has been shown that this can be attributed to an initial lack of straightness in the fiber and since in certain cases it may be necessary to predict this, a theoretical analysis of the effect has been developed. The theory has been based on well-known principles of solid mechanics. The analysis has shown that a quite small initial lack of straightness in the fiber can have a surprisingly large effect on the initial stiffness of the bearing. However the asymptotic value of the stiffness, the stiffness when the fiber is assumed to be completely straight, is actually achieved well before the fiber has completely straightened out. This is an encouraging result since the point of using fiber-reinforced bearings as isolators is to develop a lower-cost manufacturing approach than that for steel-reinforced bearings. An effort to hold the fiber tight during the vulcanization process would lead to higher costs and defeat the purpose of the endeavour.

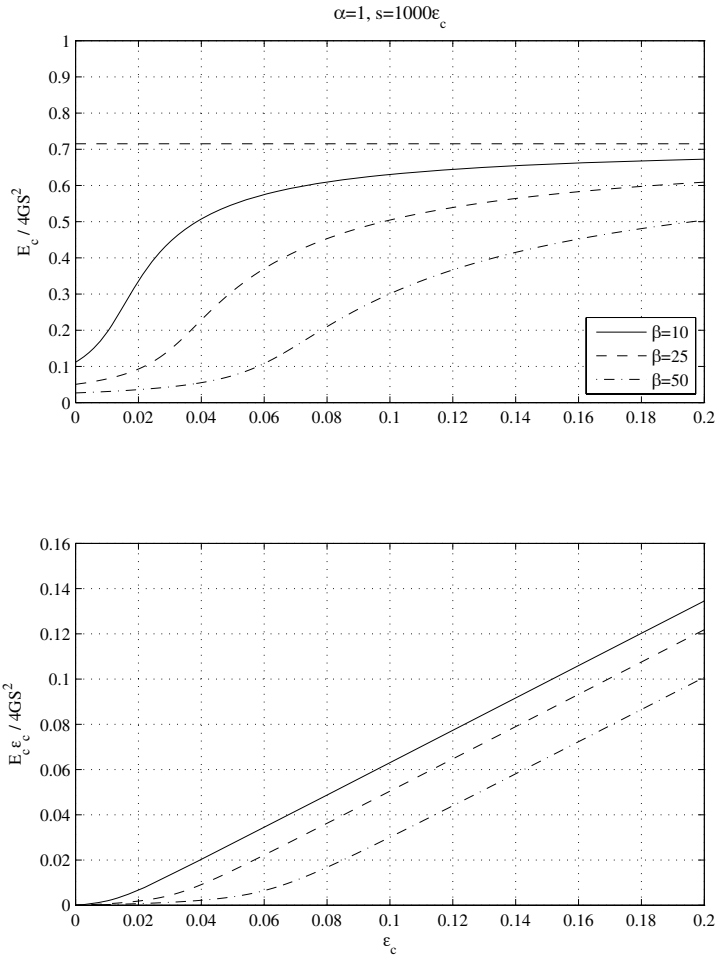


**Figure 9.** Run-in for low-stiffness fiber case: modulus and pressure vs. strain.

### References

- [Gent and Lindley 1959] A. N. Gent and P. B. Lindley, “The compression of bonded rubber blocks”, *Proceedings Institution of Mechanical Engineers* **173**:3 (1959), 111–117.
- [Gent and Meinecke 1970] A. N. Gent and E. A. Meinecke, “Compression, bending and shear of bonded rubberblocks”, *Polymer Engineering and Science* **10**:2 (1970), 48–53.
- [Kelly 1996] J. M. Kelly, *Earthquake-resistant design with rubber*, 2nd Edition ed., Springer-Verlag, London, 1996.
- [Kelly 1999] J. M. Kelly, “analysis of fiber-reinforced elastomeric isolators”, *Journal of Seismic Engineering* **2**:1 (1999), 19–34.
- [Kelly 2002] J. M. Kelly, “Seismic isolation systems for developing countries”, *Earthquake Spectra* **18**:3 (2002), 385–406. EERI Distinguished Lecture 2001.
- [Moon et al. 2003] B. Y. Moon, B. S. Khang, and H. S. Kim, “Mechanical property analysis and design of shock absorber system using fiber bearing by experimental method”, *JSME International Journal* **46**:1 (2003), 289–296.
- [Rocard 1937] Y. Rocard, “Note sur le calcul des propriétés élastiques des supports en caoutchouc adhérent”, *J. de Physique et le Radium* **8** (1937), 197.

[Summers et al. 2004] P. Summers, P. Jacob, P. Marti, G. Bergamo, L. Dorfmann, G. Castelliano, A. Poggianti, D. Karabalis, H. Silbe, and S. Triantafillou, "Development of new base isolation devices for application at refineries and petrochemical facilities", in *13th World Conference on Earthquake Engineering*, Vancouver, 2004. Paper No. 1036.

[Toopchi-Nezhad et al. 2007] H. Toopchi-Nezhad, M. J. Tait, and R. G. Drysdale, "Testing and modeling of square carbon fiber-reinforced elastomeric seismic isolators", *Structural Control and Health Monitoring* (2007).

Received 22 Apr 2008. Accepted 23 Jul 2008.

JAMES M. KELLY: [jmkelly@berkeley.edu](mailto:jmkelly@berkeley.edu)

1301 South 46th St., Bldg. 451, Richmond, CA 94804, United States

